ELSEVIER

Physica C 257 (1996) 86–98

PHYSICA C

NMR and magnetic susceptibility in superconducting and antiferromagnetic Ga-based cuprates $Y_{1-x}Ca_xSr_2Cu_2GaO_7$ $(0 \leq x \leq 0.3)$

Alexandre I. Rykov, Yutaka Ueda, Atsushi Goto, Hiroshi Yasuoka

Institute for Solid State Physics, The University of Tokyo, Roppongi 7-22-1, Minato-ku, Tokyo 106 , Japan

Received 19 October 1994

Abstract

Magnetic susceptibility and NMR/NQR measurements were performed on $Y_{1-x}Ca_xSr_2Cu_2GaO_7$ ($x = 0$, 0.1, 0.2, 0.3). The single phase samples annealed at 600°C under oxygen pressure of 30 MPa are superconductors with $T_c = 35$ K for $x = 0.2$ and $x = 0.3$. In spite of the presence of a small Curie-like term, we show that the spin susceptibility in the normal state increases with Ca doping and reaches the value $\chi_{spin} \approx 0.9$ cm^3/Cu-mole, which is comparable to other superconducting cuprates. From the observation of Cu zero-field resonance (AFNR) and susceptibility data the parent compound is classified as 2D antiferromagnet ($T_N = 387$ K). The transition from antiferromagnetic insulator to superconductor occurs with increasing concentration of carriers, but extends over several tens percent of Ca. The superconductivity is significantly suppressed by increasing disorder within limits of solubility for Ca. The Ga NQR spectra are narrow in both antiferromagnetic and superconducting regimes, but heavily broadened in the intermediate spin-glass-like domain. From $x = 0$ to $x = 0.3$, the ^{63}Cu quadrupole frequency increases from 24 to 28 MHz due to the charge transfer resulting in superconductivity. Other EFG parameters are not markedly changed from those given in $YSr_2Cu_2GaO_7$ by Pieper [Physica C190(1992)261].

1. Introduction

It is widely recognized that the strong correlations between charge carriers are a prerequisite for the occurrence of superconductivity of layered cuprates [1]. Several p-type cuprate superconductors exhibit a chemical and structural stability under withdrawal of holes. The existence of parent compounds in these systems is also attributed to the correlation effect which yields an insulating antiferromagnetic (AF) state. Therefore, the materials showing a transition from itinerant behavior to a local moment system provide a remarkable opportunity for understanding the origin of superconductivity. Among them is the double layered Ga-based cuprate $YSr_2Cu_2GaO_7$, in which holes can be generated by replacing Y with Ca [2–4]. In spite of well established superconducting properties in the doped material, the existing experimental evidence for the AF order in the parent compound is contradictory [5,6]. No long range magnetic order in $YSr_2Cu_2GaO_7$ has been observed by neutron diffraction [2,4] and an interpretation of the available experimental data on the static susceptibility is that the antiferromagnetic order is absent above 4 K [5]. Zero-field NMR [6] revealed a quadrupole split magnetic pattern at 1.2 K, which, however, showed a significant inhomogeneous broadening. Mössbauer spectroscopy [7–9] detected an antiferro-

SSDI 0921-4534(95)00565-X

magnetic order of Cu-spins by using diluted probe ^{57}Fe, but again paramagnetic behavior in susceptibility between 4 and 100 K has been reported [7]. Throughout the itinerant regime in $Y_{1-x}Ca_xSr_2Cu_2GaO_7$ with $x > 0.2$, there are no experimental data for Cu or Ga NMR spectra. A Mössbauer study of the superconducting material showed the presence of two subspectra, one of which is magnetically split [7]. Such a coexistence of superconducting and magnetic components clearly suggests the phase separation. The major question to be addressed concerning the Ca-doped sample is whether the phase separation in the superconducting material arises from Cu replacing with ^{57}Fe or it occurs even in clean iron-free material. The key role in deciding such questions must belong to an NMR investigation of the microscopic magnetic character by host nuclear probes ^{63}Cu/^{65}Cu and ^{69}Ga/^{71}Ga.

It is remarkable that the superconducting CuO_2 bilayers in the Ga-based cuprate are similar to those of $YBa_2Cu_3O_7$, though they acquire holes in a different way. Regarding the difference between structures of $YSr_2Cu_2GaO_7$ and $YBa_2Cu_3O_7$, the role of the Ga^{3+} ion residing at the similar to Cu(1) site is twofold. First, an isotropic tetrahedral coordination is preferential for the Ga^{3+} ion having a closed d^{10} shell; that is why the GaO_4 tetrahedron replaces the standard planar $Cu(1)O_4$ group. Second, due to stable valency Ga retains the oxygen stoichiometry at the nearly constant value, which is conventionally considered as "O_7." However, properties of this material are known to depend dramatically on reducing or oxidizing conditions applied on the step of synthesis [2–5,10–13]. In this paper, we study both insulating and metallic regimes in the samples prepared under different thermal treatments.

The superconductivity is known to appear in $Y_{1-x}Ca_xSr_2Cu_2GaO_7$ at the level of Ca doping $x > 0.15$–0.20, but only after synthesizing under elevated oxygen pressure [2,3,5]. Recently, superconductivity was observed up to $x = 1$ in the multiphase samples synthesized under $P = 9$ GPa at 950°C [11–13]. We observed that single phase superconducting samples can be prepared for $0.15 < x < 0.3$ using a post-anneal under fairly moderate oxygen gas pressure and temperature (30 MPa at 600°C). The intercalation of a minuscule amount of oxygen at the last stage (0.02–0.03 oxygen atoms per formula unit) is the most probable factor that governs the charge redistribution resulting in superconductivity. Within the limits of Ca-solubility, a strong tendency for charge localization remains, so that the superconducting volume fractions V_s do not exceed a few percent in the single phase materials [2,5]. It is an increase of Ca content that allows V_s to increase in multiphase samples[11–13]. In spite of significant efforts [14], the question why in the single phase range ($x < 0.3$) superconductivity can be achieved only after high-pressure oxygen loading has not yet been solved. In this respect, it is helpful to elucidate how the density of mobile carriers changes with oxygen loading. Dabrowski et al. observed that the resistance shows a metallic-like behavior in the well-oxidized samples [5]. Another property linked more directly with the carrier density in the bulk of material is the spin susceptibility. In the high-T_c superconductors, a common relation between density of carriers and spin susceptibility has been reported [15]. Therefore, the measurements of susceptibility in the normal state provide an information about the bulk carrier density and offer a test of the bulk character of superconductivity. Our analysis of spin susceptibility involves both superconducting and insulating samples prepared with a special care for eliminating magnetic impurities.

2. Experimental

2.1. Sample preparation

A series of samples of $Y_{1-x}Ca_xSr_2Cu_2GaO_7$ was synthesized for $x = 0$, 0.1, 0.15, 0.2, 0.25, 0.3 and 0.35 by usual solid state reaction of the pelletized mixture of Y_2O_3, $CaCO_3$, $SrCO_3$, CuO and Ga_2O_3. The purity of starting oxides and carbonates was at least 4N. The pellets were calcined in air at 900°C, reground and fired in air at 980–1030°C for a week with several intermediate grindings. Post-annealing was done in a pure oxygen atmosphere ($P = 24$–30 MPa) at 600°C. This resulted in superconductivity ($T_c = 20$–40 K) for $x > 0.15$. The detailed X-ray diffraction data obtained with a rotating anode reproducibly showed the phase purity of all the compositions below $x = 0.35$, except the samples with $x = 0$. Only for these Ca-free samples, the X-ray diffraction

analysis reveals the presence of the impurity $Y_2Cu_2O_5$. It is noteworthy that two strongest diffraction peaks of the green phase $Y_2Cu_2O_5$ overlaps with the reflections of $YSr_2Cu_2GaO_7$; however, the intensity of the reflection {008} of the main phase $YSr_2Cu_2GaO_7$ is extremely weak (zero). An observation of such a reflection indeed signifies the presence of $Y_2Cu_2O_5$. To obtain the single phase $YSr_2Cu_2GaO_7$ we tested several diverse synthesis conditions varying the gas atmosphere and temperature in the range 900–1100°C. It has been found from these experience that taking the reagents in a stoichiometric proportion cannot result in a single phase. The impurity of green phase $Y_2Cu_2O_5$ [16] was observed in samples synthesized under air or oxygen flow, while synthesis in the atmosphere of reduced partial oxygen pressure leads to the presence in the samples of Y_2O_3. Allowing the yttrium deficiency of 0.5% in the starting composition, we prepared in the atmosphere of 1%O_2–99%Ar at 1000°C the single phase product. Due to the absence of paramagnetic impurity $Y_2Cu_2O_5$ this sample showed the lowest magnetic susceptibility and was used in the NMR measurements.

A search for superconductivity and antiferromagnetic ordering has been performed also in the series $YSr_2Cu_{2+z}Ga_zO_{7-\delta}$ ($z = 0.1,0.2,0.3,0.4,0.5$) and $Y_{1-x}Ca_xSr_2Cu_{2+z}Ga_{1-z}O_{7-\delta}$ ($x = 0.25$, $z = 0.2$ and $x = 0.25$, $z = 0.5$), prepared in the same way and treated under similar oxygen pressure. However, neither superconductivity, nor long-range AF order were observed in these samples.

The main set of data involves six samples. Four of them belong to a series $Y_{1-x}Ca_xSr_2Cu_2GaO_7$ with x ranging from 0 to 0.3. The sample with $x = 0$ was obtained by special procedure as described above. The samples with $x = 0.1,0.2,0.3$ were obtained by high-pressure post-annealing in O_2 at 600°C. For $x = 0.2$ and $x = 0.3$, they are superconductors with $T_c = 35$ K. Unless it is mentioned, we report hereafter the results obtained on the series of samples annealed under high pressure of oxygen. To explore the role of the high-pressure annealing in O_2, two additional non-superconducting samples for $x = 0.2$ were prepared by using a treatment in O_2 and Ar flow at ambient pressure ($T = 600$°C). The oxygen contents in these samples were compared using thermogravimetry.

2.2. NMR and magnetic susceptibility

The magnetic susceptibility was measured by a SQUID magnetometer in an applied field of 1 T and temperature range from 5 to 300 K. The determination of the Neel point in the antiferromagnetic sample ($x = 0$) has been performed from the susceptibility curve measured at 1 T in the high-temperature SQUID setting. The measurements of superconducting properties were done in a field of 10 Oe, which also served for a test of absence of a ferromagnetic impurity. Thermomagnetic irreversibility below 15 K and weak ferromagnetism were indicative of the impure samples, in which the traces of $Y_2Cu_2O_5$ were correlated with X-ray diffraction data. To ensure the selection of high quality clean materials, the magnetization curves were measured up to 5 T.

The Ga NQR spectra were measured through the amplitude of quadrupolar echo by using a conventional non-coherent type pulsed spectrometer. The same technique was used for measurements of the Cu antiferromagnetic nuclear resonance (AFNR). The quadrupolar echo signal was searched in the frequency range between 10 and 110 MHz. Field-swept NMR spectra were obtained by a coherent type pulsed spectrometer with a 12-tesla superconducting magnet.

The spin–lattice relaxation time (T_1) was studied by measuring the spin echo amplitude of the NQR line as a function of the time delay between the first and second pulses in a three-pulse π–$1/2\pi$–π-sequence with a coherent type pulsed spectrometer.

3. Results

3.1. Magnetic susceptibility

The analysis of spin susceptibility consists of partition of the total susceptibility on several terms including Curie–Weiss, diamagnetic core, and orbital terms. The raw experimental susceptibility curves χ vs. T of the four samples with x varying from 0 to 0.3 are shown in Fig. 1. The χ values increase as x increases except in the small region below about $T = 50$ K for the samples with $x = 0.2$ (closed circles) and $x = 0.3$ (closed squares), in

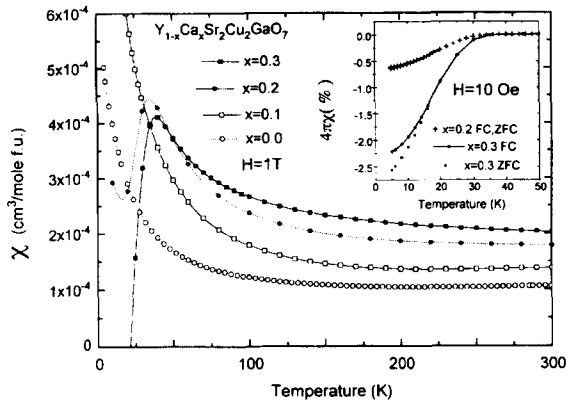

Fig. 1. Magnetic susceptibility M/H in $Y_{1-x}Ca_xSr_2Cu_2GaO_7$ measured at $H = 1$ T is shown as a function of temperature for x from 0 to 0.3. All samples but one were annealed at 600°C in pure oxygen ($P = 30$ MPa). The Ca-free sample ($x = 0$) was synthesized and cooled in the reducing atmosphere (99%Ar–1%O_2) at ambient pressure. Inset: zero-field cooled (ZFC) and field-cooled (FC) susceptibilities measured at 10 Oe for $x = 0.2$ and $x = 0.3$.

which $\chi(T)$ drops due to the onset of superconductivity. A tentative fit (Fig. 2) of $\chi(T)$ with Curie–Weiss law shows $\chi_0 + C/(T - \Theta)$ that this increase is mainly due to increasing the temperature-independent background χ_0, but not due to an increase of the Curie constant C. However, Fig. 2 demonstrates that such fits are not appropriate in the full temperature range. The $\chi^{-1}(T)$ curves clearly show maxima at 220 K for the samples $x = 0$ (open circles) and $x = 0.1$ (open squares). Therefore, we represent the susceptibility by a superposition of two constituents whose dependence on temperature are opposite to each other. Similar representations have been worked out in previous analyses of $\chi(T)$ in $YBa_2Cu_3O_{6+y}$ [17–24]. The smooth background increasing with temperature (for example, linearly, $\sim AT$) is typically expected for susceptibility in the Neel state of the low-dimensional systems. The part decreasing with T is a conventional Curie–Weiss-like term $C/(T - \Theta)$. It originates from the Cu moments whose exact location is not well known, but conventionally ascribed to an impurity phase [17–19] or to Cu^{2+} ions residing in $YBa_2Cu_3O_{6+y}$ at the Cu(1) site [20,21]. This term is extrinsic in the superconducting domain of the phase diagram for $y > 0.4$ [25]. However, at least, a part of the Curie term can be considered as intrinsic one for the y range $0 < y < 0.4$, in which the localization phenomena are likely [20–23]. Moreover, a recent observation of the strong (Cu(2)-like) anisotropy of the Curie term [24] allows us to conjecture that it originates from the Cu(2) sites. As mentioned above we have taken special care to exclude the magnetic impurities and no impurity has been found by X-ray diffraction. Therefore, the Cu^{2+} ions sitting on the Ga site or stray localized moments at the Cu site are responsible for the Curie term. It is physically plausible to suppose that the local moments are diluted and their interactions are small. In this case, the Curie–Weiss term can be approximated by a simple form C/T, which is further subtracted from the original data. To estimate the Curie constant we employed various procedures, which gave essentially the same result. For example,

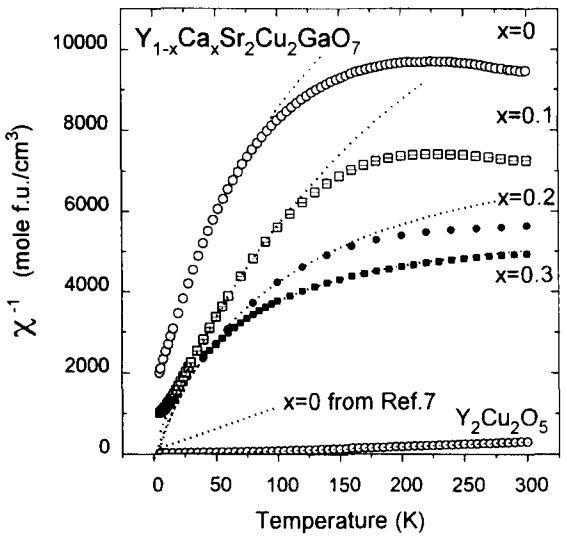

Fig. 2. Inverse magnetic susceptibility for $Y_{1-x}Ca_xSr_2Cu_2GaO_7$ samples. The symbols are the same as in Fig. 1. The dotted curves shows a Curie–Weiss law $\chi = \chi_0 + C/(T - \Theta)$ fitted to the data points in the low temperature region. The slope of fit near $T = 0$ is equal to the Curie constant C, while the curvature of fit reflects the temperature independent contribution χ_0. The deviation of fit from the data indicates the presence of third term rising with temperature. Note, that the data for $x = 0.3$ could be well fitted with Curie–Weiss low $\chi = \chi_0 + C/(T - \Theta)$ in the full temperature range above $T_c = 40$ K. Also shown for comparison of the slopes are the χ^{-1} data for $x = 0$ from Ref.[7] and χ^{-1} data for typical paramagnetic impurity $Y_2Cu_2O_5$.

Table 1
Least-squares fitting parameters χ_0, C and A from Eq. (1) for susceptibilities of$Y_{1-x}Ca_xSr_2Cu_2GaO_7$. Units are as follows: χ_0, 10^{-4} cm^3/mole f.u; C, 10^{-4} K cm^3/mole f.u. (the corresponding concentration of the free Cu^{2+} ions with a supposed magnetic moment of 1 μ_B is shown in brackets); A, 10^{-7} $K^{-1}cm^3$/mole f.u; Θ, K

	Fitting form $\chi(T) = \chi_0 + AT + C/T$			Fitting form $\chi(T) = \chi_0 + AT + C/(T-\Theta)$			
x	χ_0	C	A	χ_0	C	A	Θ
0.0 [a]	0.58	53(1.42)	0.99	0.45	69(1.85)	1.29	-8.58
0.1 [b]	0.22	130(3.48)	2.42	0.12	142(3.80)	2.64	-2.70
0.2 [b]	0.75	142(3.79)	1.93	0.86	129(3.43)	1.68	3.85
0.3 [b]	1.54	107(2.88)	0.42	1.60	101(2.72)	0.29	1.80
0.2 [c]	0.32	185(4.93)	2.34	0.31	187(4.98)	2.37	-0.36
0.2 [d]	0.37	268(7.16)	2.23	0.18	289(7.72)	2.69	-2.31

[a] The sample synthesized and cooled down under flow of mixture of 1% O_2 and 99%Ar.
[b] The samples annealed at 600°C under pure oxygen gas pressure $P = 3 \times 10^7$ Pa.
[c] The sample annealed at 600°C under ambient pressure in the flow of pure oxygen gas.
[d] The sample annealed at 600°C under Ar flow.

very close values of the Curie constant were obtained from the fit of the $\chi(T)$ curves in the range between 25 and 300 K using either form $\chi(T) = \chi_0 + AT + C/T$ or $\chi(T) = \chi_0 + AT + BT^2 + C/T$. When the Weiss constant Θ is introduced in the fitting form

$$\chi(T) = \chi_0 + AT + C/(T - \Theta) \quad (1)$$

its fitted value remains small. We show in Table 1 that the values of fitting parameters C and A are almost independent of the fitting function. The change in the constant term is also small when being considered relatively to the large negative value of $\chi_{dia} = -1.44 \times 10^{-4}$ cm^3/mole f.u. [26]. Fig. 3 shows the residual part in susceptibility after subtraction of the Curie contribution $C/(T - \Theta)$ $(\Theta \neq 0)$. It is worth mentioning that the behavior of the residual susceptibility above 25 K close to the law $\chi_0 + AT$ is not assumed in our analysis, but obtained as a result of subtraction of the Curie term from the raw data. This result can be obtained also by trial and error, by varying the Curie constant in the subtracted term and claiming that the residual part should show no Curie-like character of either sign in the range between 25 and 300 K. Such residual Curie-like behavior, if present, is smooth and cannot account for the abrupt fall in the residual term observed below 25 K. Neither function could fit the data below 25 K available in the non-superconducting samples. The abrupt fall at $T < 25$ K in the non-superconducting samples can result either from an overestimation below 25 K of the "Curie" term, in which the point $T = 25$ K corresponds to an onset of the spin-glass-like transition [27], or from the pres-

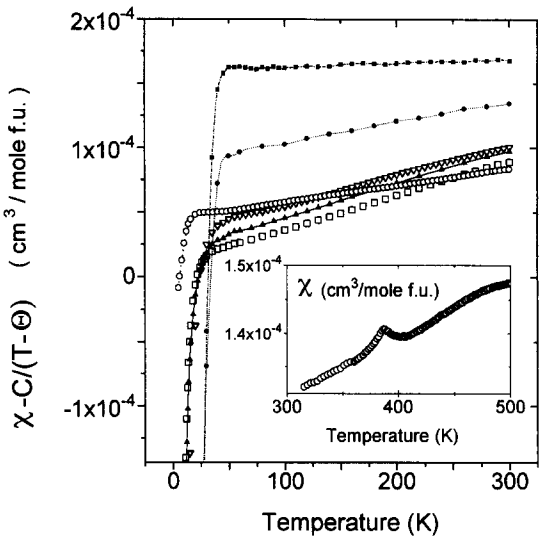

Fig. 3. The residual magnetic susceptibility of $Y_{1-x}Ca_xSr_2Cu_2GaO_7$ obtained by subtraction of the Curie–Weiss-like term $C/(T - \Theta)$ from measured data. The symbols for four samples are the same as in Figs. 1 and 2. Also shown are the $\chi - C/(T - \Theta)$ data for two other (non-superconducting) samples with Ca content $x = 0.2$. These samples were annealed at 600°C in oxygen flow (open triangles) and in Ar flow (closed triangles) and show enhanced Curie–Weiss-like contribution. The parameters C and Θ are shown in Table 1. The bottom of figure is chosen at $\chi_{dia} = -1.44$ cm^3/mole f.u. The inset illustrates the AF ordering in the sample with $x = 0$ at $T_N = 387$ K.

ence of the traces (p.p.m.) of superconductivity. Though the latter possibility was accepted in the interpretation of the similar $\chi(T) - C/T$ data in $YBa_2Cu_3O_{6+y}$ [17], the former cannot be discarded in our case.

What is of greater importance for our analysis is the behavior of spin susceptibility as a function of the doping rate above T_c. Table 1 and Fig. 3 also show the data for two additional non-superconducting samples with Ca content $x = 0.2$. These samples are prepared by treatments at ambient pressure in the flow of Ar gas (closed triangles) and O_2 (open triangles). These two specimens exhibit strongly enhanced Curie–Weiss term (Table 1), which is most likely caused by disorder related to oxygen deficiency. From our thermogravimetric measurements, the samples treated at high pressure (30 MPa) and at ambient pressure in O_2 differ by 0.026 of oxygen atoms per formula unit. This value corresponds to an effective level of Ca doping of $x_{eff} = 0.2 - 2 \times 0.026 = 0.148$. One observes in Fig. 3 that this estimate of x_{eff} is consistent with the level of residual susceptibility between those for stoichiometric (treated at oxygen pressure) samples with $x = 0.1$ and $x = 0.2$. A similar situation takes place for the Ar-treated sample with $x = 0.2$. Thus, the estimated doping level in the oxygen-deficient samples is in accordance with the trends in their susceptibilities.

In the Ca-free sample, χ_0 is clearly higher than that in Ca-doped non-superconducting samples. This peculiarity is likely related to the long-range AF order in the parent compound, while the Neel state is destroyed and only short-range AF correlations persist in the Ca-doped samples. This result is also in agreement with the fact that both Curie term and remaining part are intrinsic in the Ca-doped samples. In contrast, the intrinsic Curie term would be absent in an ideal case of parent compound. We attribute the Curie term in the Ca-free sample to some extrinsic lattice defects, which will be discussed below.

The evolution of $\chi(T) - C/(T - \Theta)$ with increasing Ca content reflects a transition between 2D antiferromagnetic and metallic states. The relative temperature dependence of $\chi(T) - C/(T - \Theta)$ is weak for two extremes: $x = 0$ and $x = 0.3$. Such behavior is reminiscent to that observed in $YBa_2Cu_3O_{6+y}$ for $y = 0$ and $y = 1$ [17–24]. For more detailed comparison the residual susceptibilities would be partitioned into spin and orbital paramagnetisms and core diamagnetism [28]:

$$\chi(T) - C/T = 2\left(\chi_{spin}(T) + \chi_{orb}\right) + \chi_{dia}, \qquad (2)$$

where χ_{spin} and χ_{orb} are values per Cu mole. The χ_{orb} depends mainly on the structure of the CuO_2 bilayers. We can separate the temperature-dependent $\chi_{spin}(T)$ and the constant χ_{orb} assuming that χ_{orb} is the same as in $YBa_2Cu_3O_7$: $\chi_{orb} = 0.585 \times 10^{-4}$ cm^3/Cu-mole[28]. After subtracting the diamagnetic contribution of core electrons: $\chi_{dia} = -1.44 \times 10^{-4}$ cm^3/Cu-mole [26] and χ_{orb}, we get the isotropic $\chi_{spin}(T) = (\chi(T) - C/T - \chi_{dia})/2 - \chi_{orb}$. For $x = 0$, the Curie contribution at 300 K is about 20% (see Fig. 1) and $\chi_{spin} = 0.53 \times 10^{-4}$ cm^3/Cu-mole. This number is close to the corresponding quantity for $YBa_2Cu_3O_6$ at 300 K, $\chi_{spin}^{1236} = 0.5 \times 10^{-4}$ cm^3/Cu-mole, calculated using the data of Ref. [20]. The theoretical value of 0.48×10^{-4} cm^3/Cu-mole for 2D $S = 1/2$ Heisenberg model [29] agrees with our data as well. For $x = 0.3$, the obtained χ_{spin} value at 300 K is 0.95×10^{-4} cm^3/Cu-mole, which is equal within experimental accuracy to an identical quantity in $YBa_2Cu_3O_7$ [27]. At the intermediate doping levels, the increased slope of the curve $\chi(T) - C/T$ vs T is observed. The rapid decrease of spin susceptibility with lowering temperature is typical in the underdoped superconducting systems. The underdoped regime is characterized by enhanced antiferromagnetic fluctuations, which start to develop far above T_c, as it was revealed by studies of Cu relaxation rate $1/T_1$ [1,27,29]. In the non-superconducting regime, we observe that the slope in the temperature dependence of χ_{spin} is also comparatively large. Therefore, the strong temperature dependence of χ_{spin} is not necessarily related to the underdoped superconducting region. We show in the inset of Fig. 3 that the magnetic susceptibility in the antiferromagnetic sample ($x = 0$) increases above the Neel temperature $T_N = 387$ K as well as below it. The underlying model of the Heisenberg $S = 1/2$ 2D-antiferromagnet with a coupling constant J predicts an increase of χ_{spin} with increasing temperature up to $T \approx J/k_B \sim 10^3$ K; the slope A is related to the spin stiffness ρ_s ($A \sim \rho_s^{-1}$) [29]. However, susceptibility behavior seems to be more complicated in the intermediate spin-glass-like domain. The problem theoret-

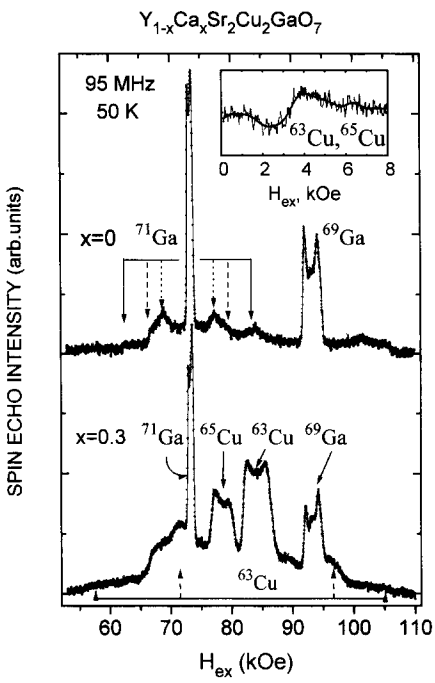

Fig. 4. NMR spectra of $YSr_2Cu_2GaO_7$ and $Y_{0.7}Ca_{0.3}Sr_2Cu_2O_7$ taken at $\nu = 95$ MHz and $T = 50$ K. The central transition peaks $(\frac{1}{2} \leftrightarrow -\frac{1}{2})$ are indicated by the symbol of the respective nuclei. Both Ga and Cu contribute to the spectrum of the superconducting ($T_c = 35$ K) compound. The echo signal from Cu is wiped out from the field spectra of the Ca-free AF sample due to the appearance of the static hyperfine field at the Cu sites. In the AF sample, the Cu-resonance field extends over some hundreds of kG from $(H_{hf} - H)$ to $(H_{hf} + H)$. The inset shows the Cu hyperfine singularity observed in the region of the low-field boundary $H_{hf} - H$. The positions of first-order quadrupole singularities are indicated by arrows for ^{71}Ga on the upper spectrum. The solid arrows marks the singularities at $\Theta = 0$, while dashed and dotted arrows correspond to the singularities at $\Theta = \pi/2$, $\phi = \pi/2$ and $\Theta = \pi/2$, $\phi = 0$, respectively. The powder-pattern variables Θ and ϕ are the polar coordinates of the external field H in the reference of principal EFG axes. The gap beetween dotted and dashed arrows illustrates the measure of the Ga site asymmetry ($\eta = 0.22$). At the bottom of the figure, the positions of first-order quadrupole singularities for ^{63}Cu are shown ($\eta \approx 0$).

ically is that the "Curie" contribution in the non-superconducting lightly doped regime results from localization phenomena. The separate consideration of the two terms in this case has an arbitrary meaning. Our analysis in these samples clarifies the complicated shape of $\chi(T)$, which can be scarcely seen in the raw data.

3.2. NMR and NQR spectra

The energies of quadrupole and magnetic hyperfine interactions for ^{63,65}Cu and ^{69,71}Ga nuclei fall in quite comparable range due to the close values of quadrupole moments and gyromagnetic ratios. The presence of large electric field gradients (EFG) at both Cu and Ga sites results in significant overlap of Ga and Cu signals in sweeping magnetic field. However, the contributions of ^{63,65}Cu and ^{69,71}Ga resonances to the spectrum can be readily identified by comparing the spectra of parent and superconducting compounds for Ca content $x = 0$ and $x = 0.3$, respectively (Fig. 4). The two structural sites are probed by four naturally abundant species ^{69}Ga, ^{71}Ga, ^{63}Cu, ^{65}Cu. The subspectrum for each nucleus consists of a powder-broadened first-order quadrupole pattern for the satellite $(\pm 3/2 \leftrightarrow \pm 1/2)$ transition and a second order powder pattern for the central $(1/2 \leftrightarrow -1/2)$ transition. The Cu subspectrum arises only in the absence of the antiferromagnetic ordering and exhibits quadrupole splitting with $\nu_Q = 28.4$ MHz. Similarly to $YBa_2Cu_3O_7$ and other cuprates having CuO_2 planes, the quadrupole splitting is dominated by large negative contribution into EFG's principal component V_{ZZ} from the half-filled $d_{x^2-y^2}$ orbital. In spite of the closed d-shell, Ga also exhibits large splitting ($\nu_Q = 22.5$ MHz), which is purely ionic in origin. The large lattice quadrupole energy suggests

Table 2
Hyperfine parameters for Cu and Ga sites derived from NQR and NMR spectra presented in Figs. 3–6. The notation and units are as follows: $\nu_Q = eQV_{ZZ}/2h$, MHz; $\nu_L = \gamma H_{hf}$, MHz; $\eta = (V_{XX}-V_{YY})/V_{ZZ}$, Θ is the angle between hyperfine field and V_{ZZ} directions (degrees); $\nu_{NQR} = \nu_Q(1 + \eta^2/3)1/2$, MHz

x	$^{63}\nu_Q$	$^{65}\nu_Q$	$^{63}\nu_L$	$^{65}\nu_L$	η(Cu)	θ	$^{71}\nu_{NQR}$	$^{69}\nu_{NQR}$	η(Ga)
0.0	24.0(3)	22.2(5)	85.4(1) [a]	91.5(1) [a]	0.06(10)	90(5)	14.20(2)	22.49(1)	0.2(1)
0.3	28(1)	26(2)	–	–	0.0(1)	–	14.24(8)	22.42(3)	0.22(2)

[a] The corresponding value of H_{hf} is 75.7 kOe.

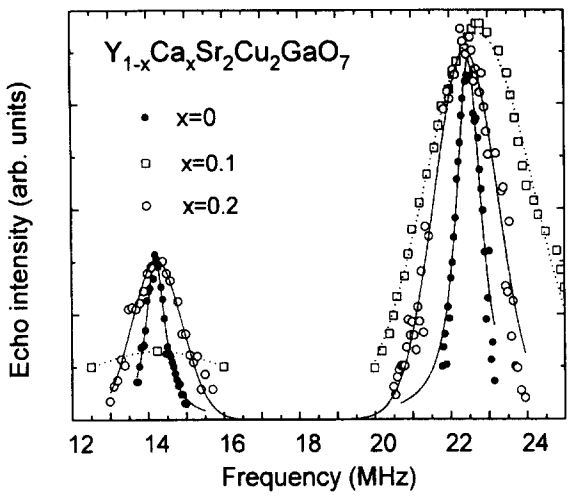

Fig. 5. The Ga NQR spectra for $x = 0$, 0.1 and 0.2 in $Y_{1-x}Ca_xSr_2Cu_2GaO_7$ at 1.4K. The intensity is normalized to the same scale for different samples without correction on the overall ν^2-dependence. The spectrum of ^{71}Ga NQR for Ca content $x = 0.1$ is shown schematically because of extremely low intensity of the echo signal at this line. The Ga NQR spectrum for $x = 0.3$ (not shown) is not markedly changed in linewidth from that for $x = 0.2$.

that the symmetry of the tetrahedral Ga site is far from the cubic one; the GaO_4 tetrahedron is strongly compressed between the adjacent CuO_2 bilayers [9]. The central $1/2 \leftrightarrow -1/2$ peaks for both Ga and Cu sites appear in split form. This suggests that the asymmetries of the electric field gradient (EFG), η, in either site are small. The hyperfine parameters derived from the spectra are summarized in Table 2.

A comparison of the lineshapes for the Ga and Cu central $1/2 \leftrightarrow -1/2$ peaks shows extra broadening for Cu resonance with respect to Ga resonance. This extra broadening is consistent with the fact that Cu signal is missing in the NQR spectrum at the frequency $\nu_Q = 28.4$ MHz. In contrast, the Ga NQR signal has been found in all the samples, though the intensities and linewidths of the Ga NQR spectra depend on the Ca content (Fig. 5). The sharpest profile of the Ga resonance was obtained for the antiferromagnetic sample ($x = 0$). The small linewidth means that the dipolar fields from adjacent Cu spins are nearly canceled at the Ga site. This result is in agreement with the previous suggestion of Pieper of the similarity between magnetic structures of $YBa_2Cu_3O_6$ and $YSr_2Cu_2GaO_7$ [6]. We also observed that the Ca substitution leads to a decrease of Ga intensities, however, contrary to the Pieper's report (Ref. [6]), the change in linewidths revealed itself as well. Observe in Fig. 5, with increasing x from $x = 0$ to $x = 0.1$ the linewidth first increases, but further increasing of the Ca content to $x = 0.2$ lead to a decrease of the linewidth. The increase in the linewidth at the first stage can be explained by magnetic effects. The ^{71}Ga resonance has been observed in the $x = 0.1$ sample with very low intensity. This is consistent with large magnetic contribution to the linewidth for ^{71}Ga, which has a smaller Q but larger γ than ^{69}Ga. Our susceptibility data suggest that the doping level $x = 0.1$ corresponds to the spin-glass regime. Broadening in the Ga NQR line with increasing x is similar to that for the $Cu(1)_2$ NQR line in the antiferromagnetic $YBa_2Cu_3O_{6+y}$ as oxygen content y increases (the subscript in $Cu(1)_2$ denotes here the oxygen coordination number) [30]. The long range AF is known to disappear at $y = 0.4$ in $YBa_2Cu_3O_{6+y}$. In such a wide AF domain, the charge is not directly transferred to the CuO_2 planes. While there is only one Cu site in the Ga-based cuprate, the holes are introduced immediately into CuO_2 planes. Therefore, an abrupt breakdown of the AF order is expected when holes are generated by cationic substitution. A spin-glass-like magnetic ordering forms in the intermediate region between AF and superconductivity. A level of doping appropriate to the spin-glass regime extends for cationic substitution in $La_{2-z}Sr_zCuO_4$ from $z = 0.02$ to $z = 0.08$. Similar levels of doping correspond to x values of 0.04 and 0.16 in $Y_{1-x}Ca_xSr_2Cu_2GaO_7$. The NQR data suggest that the cancellation of the magnetic field at Ga site breaks down for $x = 0.1$ and the Ga-line becomes broadened and shifted toward higher frequency. We estimate the average dipolar field as 3 kOe from the extra width of the ^{69}Ga line. When superconductivity appears with further increasing Ca content, the shift vanishes and the width decreases. The residual linewidth results from purely quadrupolar broadening, caused by distribution of EFG over Ga sites having different number of Ca neighbors. For $x = 0.3$, Ga resonance show no changes compared with $x = 0.2$.

The spectra measured by the zero-field NMR in the antiferromagnetic regime (AFNR-spectra) reveal inhomogeneous line broadening similar to that re-

ported previously [6]. However, we observed that the quality of spectra can be significantly improved by using the above-mentioned treatment in a reducing atmosphere (99%Ar–1%O_2). Fig. 6 shows the spectrum of our high-quality sample ($x = 0$). Pieper attributed the broadening in both Ga and Cu resonances of $GdSr_2Cu_2GaO_7$ to the defects in the rare earth sublattice [6]. We observed that broadening of Cu AFNR spectra increases in the presence of $Y_2Cu_2O_5$ impurity. These facts could be understood to be consistent with Pieper's suggestion if we suppose that the increasing concentration of Y defects in the matrix leads to the formation of impurity phase. Raising the temperature up to 4.2 K leads to a significant decrease of intensity but has no effect on the line positions. The Cu signal usually disappears below 77 K, most probably, due to shortening of the spin–lattice relaxation times and hyperfine field inhomogeneity. The average hyperfine field $H_{hf} = 75.7$ kOe showed no change in our temperature range. Along with field-swept NMR spectra and susceptibility data this fact means that $YSr_2Cu_2GaO_7$ exemplifies two-dimensional antiferromagnet with Neel temperature $T_N = 387$ K. This value of Neel temperature is quite close to the magnetic ordering temperature of 420 K in the Fe-based isostructural compound [8]. When diamagnetic Ga is fully replaced by magnetic Fe ($S = 5/2$) [8,9], the T_N value remains nearly unaffected by a huge change of the interbilayer Cu–Cu coupling. This fact strongly suggests

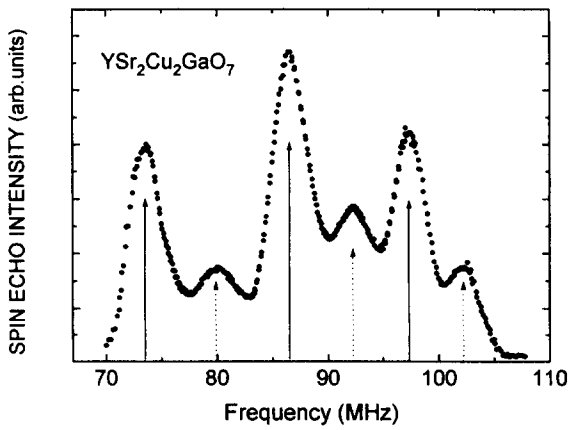

Fig. 6. AFNR spectrum of $YSr_2Cu_2GaO_7$ at 1.4 K. The sample has been prepared in the reducing atmosphere (1%O2–99%Ar) at 1000°C. The solid and dashed arrows show the positions of ^{63}Cu and ^{65}Cu lines, respectively.

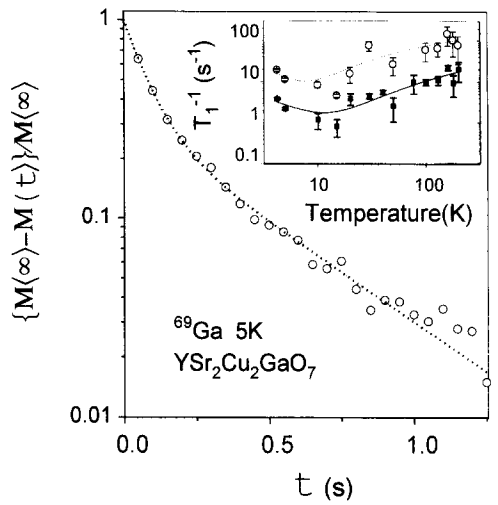

Fig. 7. Typical behavior of the ^{69}Ga nuclear magnetization. The relaxation curve is shown for NQR line in $YSr_2Cu_2GaO_7$ at 5 K. An inset shows the temperature dependence of ^{69}Ga relaxation rate. The solid and open symbols in the inset correspond to the relaxation rate of the Ga sites away and near structural imperfections, respectively.

the 2D-character of the AF ordering in both Ga- and Fe-based cuprates.

In the high-quality antiferromagnetic samples, ^{63,65}Cu AFNR line narrowing is accompanied by a decrease of spin–lattice relaxation rates of ^{69}Ga. The average relaxation time $^{69}T_1$ was increased by one or two orders of magnitude in the clean sample prepared by the above-mentioned reducing treatment. It was observed that such a slow relaxation cannot be described by a recovery curve of a single exponential type. For a quantitative analysis, the recovery curves were represented by two exponential decay components (Fig. 7). Such a crude analysis involves a model, in which the short component is attributed to the Ga sites located near defects, while the long component reflects the intrinsic relaxation process. The temperature dependencies for both components are weak and roughly similar (see inset in Fig. 7). Since Ga site experiences a rough cancellation of dipolar field from neighboring Cu spins, which are ordered below T_N, the intrinsic ^{71,69}Ga relaxation rate is not a faithful probe of magnetic excitations on the Cu ions. The cancellation condition is broken in some vicinity of either lattice defect or trapped doping hole. Such Ga sites are influenced by excitations of neighboring Cu spins. The high sensitivity of the

interbilayer Ga-site to the breakdown of symmetry in the Cu spin alignment explains the large (at least about a factor of ten) difference between long and short components in $^{69}T_1$.

The measurements of the ^{69}Ga relaxation rate in the superconducting samples have revealed its rough temperature independence in the range between 4.2 and 80 K and even slight decrease with temperature above T_c. Here again the recovery of the nuclear magnetization is described by overlapping two decays. Above T_c, the long T_1 (= 0.14 s) for the slow decay component indicates that there is an extremely weak coupling of the ^{69}Ga probe to the conduction band electrons. The search for the Cu NQR signal in this highly disordered system remains an issue for further work.

4. Discussion

This study showed the features of the 2D antiferromagnet for the cuprate $YSr_2Cu_2GaO_7$, in which superconductivity by a common way follows from p-type doping. While the carrier density is large enough for the bulk superconductivity, the question arises as to why the volume fraction V_s remains small. Moreover, there exists an empirical rule that usually we are able to find the Cu quadrupolar echo in the bulk superconductors. It is reasonable to suppose that a high degree of disorder in this material is at the origin of both the poor bulk fraction and absence of the Cu NQR signal. The structural distortions are evident from the linewidth of X-ray diffraction reflections, which broadens dramatically with Ca-doping, especially, at high diffraction angles. The strains induced by cationic substitution are correlated with the site occupancy by foreign dopants. For the same level of p-doping, the occupancy of the Y site by Ca in $Y_{1-x}Ca_xSr_2Cu_2GaO_7$ is four times higher than the occupancy of the La site by Sr in $La_{2-z}Sr_zCuO_4$. That is why structural distortions in the CuO_2 planes of Ga-based cuprate develops far below the Ca solubility limit, which is large enough for occurrence of superconductivity.

Another possible reason for the missing Cu NQR and lack of Meissner fraction is linked with extrinsic lattice defects unrelated to doping. It is worth mentioning three types of such unintentional defects.

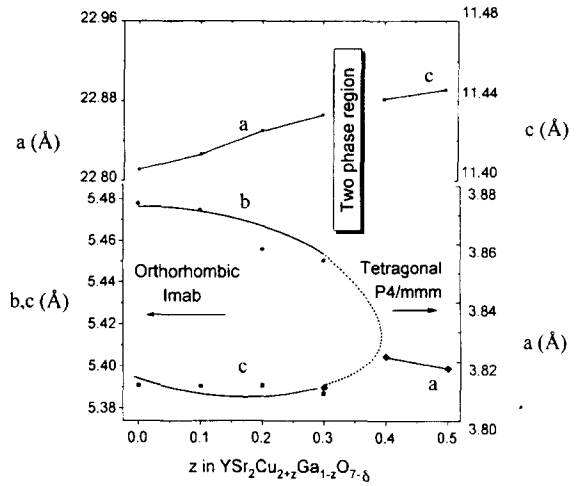

Fig. 8. Compositional dependence of the lattice parameters for $YSr_2Cu_{2+z}Ga_{1-5z}O_7$. Note a region of coexistence of orthorhombic and tetragonal phases near $z = 0.3$. The scales on both right and left axes are chosen according to the relationships: $a_{Ima2} \approx 2c_{P4/mmm}$; $b_{Ima2} \approx \sqrt{2}a_{P4/mmm}$; $c_{Ima2} \approx \sqrt{2}a_{P4/mmm}$. The lines are guides to the eye.

These three variety of disorder occur, respectively, in A, B and O sublattices of the primary perovskite structure ABO_3. The sublattice of small-size cations (in perovskite notation B) undergoes orientational disordering in the arrangements of Ga–O chains. One discerns two orientations of the chain buckling [32]. A change between different orientations occurs due to the presence of Cu at the Ga site [8]. Since the Cu^{2+} ion tends to have the square planar oxygen coordination, it would disrupt the chains of the GaO_4 tetrahedra. We synthesized a series of solid solutions $YSr_2Cu_{2+z}Ga_{1-z}O_7$ up to $z = 0.5$ and observed the transition from orthorhombic to tetragonal symmetry near $x = 0.3$ (Fig. 8). Neither Ga NQR nor Cu AFNR spectra were found in the samples of this series. The procedure of post-annealing at the oxygen pressure described above did not allow superconductivity in Ca-doped samples with z ranging from 0.1 to 0.5 to be achieved. In the same way, the disordered tetragonal oxide $YSrBaCu_{2.5}B_{0.5}O_7$ [31] is not a superconductor. Therefore, the substitution of Ga by Cu is unfavorable for superconductivity. Since some Cu ions are supposed to reside at the Ga site even when $z = 0$ [8], they can be considered as a detrimental factor for the superconducting properties. The large range of Cu solubility and the discontinu-

ous character of the transition from orthorhombic to tetragonal symmetry (Fig. 8) suggest that a Cu ion is stable at a Ga site. The immobility of such defects results from related topological disorder [32,8] and can be reinforced by slight deviation from cationic stoichiometry. In this respect, an exact control of composition encounters such an obstacle as the visible volatility of several oxides of gallium.

The second kind of disorder was first proposed by Pieper [6] for Ca-free composition. It involves the sublattice of rare earth element. Two possibilities exist for the missing Y in this sublattice: either cationic disorder between Y and Sr sites, or cationic vacancies [V_Y''']. In the latter case the electroneutrality condition would be fulfilled by the generation of holes. Our relaxation experiments in the parent material $YSr_2Cu_2GaO_7$ have an implication for the searching for such holes. Tomlins et al. [10] reported that the electrical conductivity and thermopower in the undoped specimens $YSr_2Cu_2GaO_7$ behave as if the samples were doped with 2% of Ca. The mobility of carriers was characterized by activation energy E_a of ~ 200 meV. The shallow carriers with $E_a = 1280$ K were recently explored by measurement relaxation rate of Cu(1) in $YBa_2Cu_3O_{6.1}$ [33]. For the Cu(1)-nuclei in $YBa_2Cu_3O_6$, Rajarajan et al. [34] observed below 60 K a temperature independent T_1 of 418 ms. A sharp peak in the relaxation rate at $T = 140$ K in $YBa_2Cu_3O_{6.1}$ has been interpreted as a manifestation of the hole motion in the CuO_2 planes [33]. The thermally activated relaxation with a peak of the Ga relaxation rate at the temperature of roughly $E_a/10$ is expected in the presence of mobile carriers [33,35]. The temperature dependence of T_1^{-1} in Fig. 7 suggests that shallow holes (< 200 K) are unlikely. The holes trapped on the lattice defects would contribute into the slow non-single-exponential relaxation, which was indeed observed in the material prepared under reducing conditions ($1\%O_2$–$99\%Ar$). On the other hand, the oxygenated sample showed a peak of the relaxation rate $^{69}T_1^{-1}$ at $T = 45$ K. However, magnetic impurities observed in the oxygenated Ca-free material may produce a contaminating contribution into the relaxation rate and the peak in $^{69}T_1^{-1}$ cannot be directly attributed to the shallow carriers.

The source of cationic defects in the (Y,Sr)-sublattice becomes more clear if the double-layer compound $YSr_2Cu_2GaO_7$ is considered along with the single-layer Ga-based cuprate $La_{1-x}Sr_{1+x}CuGaO_5$ [36]. This Ga-based cuprate has been reported to be a single phase for only a very narrow solubility range $0.10 < x < 0.13$, in which neither superconductivity nor magnetic order could occur. The impurity phases, observed outside this solution range, are different for Sr-rich and La-rich compositions [36]. In the same way, the underlying point defect structure would be different between the parent compound $YSr_2Cu_2GaO_7$ and the heavily Ca-doped material. While cationic defects are likely in the Ca-free compound, the Ca-doped material becomes susceptible to the formation of vacancies in the O-sublattice. The release of 0.026 oxygens per formula unit from superconducting material leads to a loss of superconducting properties. Therefore, we suppose that oxygen non-stoichiometry is important in the Ca-doped material, albeit small. Manthiram, Lee and Goodenough have shown that Ca doping in $Y_{1-x}Ca_xBa_2Cu_3O_{7-\delta}$ induces the release of some oxygens [37]. An actual distribution of oxygen vacancies for the Ba-case is complex and some similarity between Ba- and Sr-cases cannot be disregarded. An interesting situation takes place in the electron-doped Nd–Ce–Cu–O material, which shows a similar behavior with respect to removal/loading of oxygen. The superconductivity in this system appears after removal of similarly small excess of oxygen [38,39]. For this material, Matsuda et al. [39] proposed a speculative model explaining the strong carrier localization in the presence of oxygen defects on the sites apical with respect to CuO_2 planes. If we adopt this idea and replace an extraneous oxygen in this plausible model by a vacancy for our case, we obtain an oxygen defect in the SrO layer acting on some large enough neighborhood as a breaker of the effect of the Ca dopants. In this situation, a detrimental effect of the oxygen vacancies on superconducting properies is expected to be stronger in $Y_{1-x}Ca_xSr_2Cu_2GaO_{7-\delta}$ than in $Y_{1-x}Ca_xBa_2Cu_3O_{7-\delta}$ because of the very articulated 2D-character of superconductivity in the former compound.

The hyperfine interactions first investigated in the parent material $YSr_2Cu_2GaO_7$ by Pieper [6] exhibit in our sample close parameters, although some differences are noteworthy. Our best fit of the AFNR spectra was obtained assuming 90°-value for the angle θ between EFG's principal component V_{zz}

and H_{hf}. Such a result can be explained as follows. The H_{hf} lies in the plane of shortest cell axes. The main contribution into V_{ZZ} is coming from $d_{x^2-y^2}$ orbital which is inserted in the basal plane of the CuO_5 pyramid. This implies for V_{ZZ} a direction normal to the pyramid basal plane. Roth et al. reported a very small tilt ($\sim 2.5°$) of the pyramid basal plane with respect to cell axes [4]; this is in fair agreement with our result.

The quadrupole coupling strength of Cu increases when the structure undergoes superconductization (Table 2). We ascribe the increase of ν_Q from 24 to 28 MHz to the reduction in the lattice term in EFG caused, in turn, by decreasing apical distance. This behavior is similar to 1:2:3 and other cuprates, which can be prepared in both reduced and hole-doped states. A survey of the experimental data on the EFG observed by Cu NMR shows that the correlation between doping level and ν_Q is straightforward [40]. It is noteworthy that Mössbauer spectroscopy on the diluted ^{57}Fe probe driven into the CuO_2 plane deals with the same structural change by doping [8,41]. However, the trends in quadrupole splitting are opposite as EFG is purely ionic for $Fe^{3+}(3d^5)$.

The underlying cause of phase separation observed by Mössbauer spectroscopy in the superconducting samples [7] is extrinsic with respect to Ga-based cuprate, as it follows from the present results on NMR spectra measured by sweeping the external field. No coexistence of Cu magnetic ordering and superconductivity was observed in the Fe-free samples. A possible explanation for the result of Mössbauer experiment involves a precipitation of iron in the (magnetic) impurity phase or clustering of iron ions into rows. Since iron may enter the Cu(2) site wherein it acts in the charge state 3 + [8,9,41], the hole's location is unfavorable in the Fe vicinity. Therefore, Fe reinforces locally an exchange coupling between Cu. Thus, the magnetic ordering is likely to be induced by introducing ^{57}Fe probe.

5. Concluding remarks

In spite of the extensive studies [2–14], an evidence for bulk character of superconductivity in Ga-based cuprate remains scarce. In the earlier work [2] the converse possibility has been emphasized that a fraction of other phase can be responsible for the superconductivity occurrence. The careful preparation of antiferromagnetic compound in this work allowed to isolate its intrinsic susceptibility. This led us, in turn, to an observation of the significant susceptibility change by doping. Similarly, the clean superconducting materials showed a development of a coherent state observed by narrowing of Ga NQR.

Thus, our study demonstrates that the double layer Ga-based cuprate belongs to the family of 2D antiferromagnets, while the electronic state in the Ca-doped materials is close to metallic one, but shows a strong tendency to the localization of carriers. The metallic state develops on the background of high disorder, which is crucial for superconductivity in the underdoped regime. Both the susceptibility and NMR results support this point of view.

Acknowledgements

This work was funded by the Ministry of Education, Science and Culture of Japan. Thanks are due to Dr. A. Hayashi, K. Otzschi, M. Isobe, Yasuhiro Uyeda and T. Ohama for informative communications and assistance in experiments.

References

[1] H. Yasuoka, T. Imai and T. Shimisu, in: Strong Corelation and Superconductivity, eds. H. Fukuyama, S. Maekawa and A.P. Malozemoff, Springer Series in Material Science, Vol.89 (Springer, Berlin, 1989) p.254.

[2] J.T. Vaughey, J.P. Thiel, E.F. Hasty, D.A. Groenke, C.L. Stern, K.R. Poeppelmeier, B. Dabrowski, D.G. Hinks and A.W. Mitchell, Chem. Mater. 3 (1991) 935.

[3] R.J. Cava, R.B. Van Dover, B. Batlogg, J.J. Krajewski, L.F. Scheemeyer, T. Siegrist, B. Hessen, S.H. Chen, W.F. Peck and L.F. Rupp, Physica C 185–189 (1991) 180;S.A. Sunshine, L.R. Schneemeyer, T. Siegrist, D.C. Douglass, J.W. Waszczac, R.J. Cava, E.M. Gyorgy and D.W. Murphy, Chem. Mater. 1 (1989) 331.

[4] G. Roth, P. Adelmann, G. Heger, R. Knitter and Th. Wolf, J. Phys. (Paris) I 1, 721 (1991).

[5] B. Dabrowski, P. Radaelli, D.G. Hinks, A.W. Mitchell, J.T. Vaughey, D.A. Groenke and K.R. Poeppelmeier, Physica C 193 (1992) 63.

[6] M.W. Pieper, Physica C 190 (1992) 261.

[7] I. Felner, I. Nowik, U. Asaf, G. Yona, U. Yaron and E.R. Bauminger, Physica C 210 (1993) 55.

[8] A. Rykov, V. Caignaert, G. Van Tendeloo, J.M. Greneche, F. Studer, N. Nguyen, A.Ducouret, P. Bonville and B. Raveau, J. Solid St. Chem. 113 (1994) 94.
[9] A. Rykov, V. Caignaert and B. Raveau, J. Solid St. Chem. 109 (1994) 295.
[10] G.W. Tomlins, N.-L. Jeon, T.O. Mason, D.A. Groenke, J.T. Vaughey and K.R. Poeppelmeier, J. Solid St. Chem. 109 (1994) 338.
[11] M. Isobe, Y. Matsui and E. Takayama-Muromachi, Physica C 222 (1994) 310.
[12] M. Isobe, M. Suzuki, T. Ami, S. Fukushima and M. Tanaka, Adv. Supercond. 5 (1993) 247.
[13] M. Isobe, K. Kosuda and E. Takayama-Muromachi, Physica C 227 (1994) 351.
[14] J.P. Zhang, D.A. Groenke, B. Dabrowski, K.R. Poeppelmeier and L.D. Marks, Physica C 227 (1994) 259.
[15] Z.P. Han, R. Dupree, A. Gencten, R.S. Liu and P.P. Edwards, Phys. Rev. Lett. 69 (1992) 1256.
[16] H. Drulis, J. Klamut, A.J. Zaleski and R. Horyn, Phys. Rev. B 48 (1993) 9843.
[17] J.M. Tranquada, H. Moudden, A.L. Goldman, P. Zolliker, D.E. Cox, G. Shirane, S.K. Shinha, D. Vaknin, D.C. Johnston, M.S. Alvares, A.J. Jacobson, J.T.Lewandowski and J.M. Newsam, Phys. Rev. B 38 (1988) 2477.
[18] K. Fukuda, S. Shamoto, M. Sato and K. Oka, Solid St. Commun. 65 (1988) 1323.
[19] K. Westerholt and H. Bach, Phys. Rev. B 39 (1988) 858.
[20] Y. Nakazawa and M. Ishikawa, Physica C 158 (1989) 381.
[21] Y. Yamaguchi, M. Tokumoto, S. Waki, Y. Nakagawa and Y. Kimura, J. Phys. Soc.Jpn. 58 (1989) 2256.
[22] T. Kawagoe, T. Mizoguchi, K. Kanoda, T. Takahashi, M. Hasumi and S. Kagoshima, J. Phys. Soc. Jpn. 57 (1988) 2272.
[23] T. Takabatake, M. Ishikawa and T. Sugano, Jpn. J. Appl. Phys. 26 (1987) L1859.
[24] R.E. Walstedt, R.F. Bell, L.F. Schneemeyer, J.V. Waszczak and G.P. Espinosa, Phys. Rev. B 45 (1992) 8074.
[25] Y. Yoshinari, H. Yasuoka, Y. Ueda, K. Koga and K. Kosuge, J. Phys. Soc. Jpn. 59 (1990) 3698.
[26] This number has been calculated by replacing the partial contributions χ_{dia}(Sr) for χ_{dia}(Ba) and χ_{dia}(Ca) for χ_{dia}(Y) in the value of $\chi_{dia} = -1.66\times10^{-4}$ cm^3/mole known for $YBa_2Cu_3O_7$ from Ref. 24.
[27] F.C. Chou, F. Borsa, J.H. Cho, D.C. Johnson, A. Lascialfari, D.R. Torgeson and J. Ziolo, Phys. Rev. Lett. 71 (1993) 2323.
[28] T. Shimizu, H. Aoki, H. Yasuoka, T. Tsuda, Y. Ueda, K. Yoshimura and K. Kosuge, J. Phys. Soc. Jpn. 62 (1993) 3710.
[29] S. Chakravarty, B.I. Halperin and R.D. Nelson, Phys. Rev. B 39 (1989) 2344;A.J. Millis and H. Monien, Phys. Rev. Lett. 70 (1993) 2810;A.V. Chubukov and S. Sachdev, Phys. Rev. Lett. 71 (1993) 169.
[30] H. Yasuoka, T. Shimizu, T. Imai, S. Sasaki, Y. Ueda and K. Kosuge, Hyperfine Interactions 49 (1989) 167.
[31] W.J. Zhu et al., Physica C 205 (1993) 118.
[32] Q. Huang, R.J. Cava, A. Santoro, J.J. Krajewski and W.F. Peck, Physica C 193 (1992) 196;O. Milat, T. Krekels, G. Van Tendeloo and S. Amelinckx, J. Phys. (Paris) I 3 (1993) 1219.
[33] S.G. Jang, C. Bucci, R. De Renzi, G. Guidi, M. Varotto, C. Segre and P. Radaelli, Physica C 226 (1994) 301.
[34] A.K. Rajarajan, L.J. Gupta and R. Vijayaraghavan, Physica C 193 (1992) 413.
[35] P. Carretta, M. Corty and A. Rigamonty, Phys. Rev. B 48 (1993) 3433.
[36] J.T. Vaughey, J.B. Wiley and K.R. Poeppelmeier, Z. anorg. allg. Chem. 598/599 (1991) 327;J.T. Vaughey, R. Shumaker, S.N. Song, J.B. Ketterson and K.R. Poeppelmeier, Mol. Cryst. Liq. Cryst. 184 (1990) 335; M.T. Anderson, J.T. Vaughhey and K.R. Poeppelmeier, Chem. Mat. 5 (1993) 151.
[37] A. Manthiram, S.-J. Lee and J.B. Goodenough, J. Solid St. Chem. 73 (1988) 278.
[38] A. Nath, N.S. Kopelev, V. Chechersky, J.L. Peng, R.L. Greene, B.-h. O, M.I. Larkin and J.T. Markert, Science 265 (1994) 73.
[39] M. Matsuda, Y. Endoh, K. Yamada, H. Kojima, I. Tanaka, R.J. Birgeneau, M.A. Kastner and G. Shirane, Phys. Rev. B 45 (1992) 12548.
[40] T. Shimizu, J. Phys. Soc. Jpn. 62 (1993) 772;T. Shimizu, H. Yasuoka, T. Tsuda, K. Koga and Y. Ueda, Bull. Magn. Res. 12 (1990) 39.
[41] A. Rykov, V. Caignaert, N. Nguyen, A.Maignan, E. Suard and B. Raveau, Physica C 205 (1993) 63;I. Felner, D. Hechel, A. Rykov and B. Raveau, Phys. Rev. B 49 (1994) 686.